Broiler chickens with 1950s genetics display a stable immune profile as measured by Kinome, mRNA expression, and metabolism when stimulated early in life with CpG

Bridget A. Aylward [*], Casey N. Johnson,[*] Famatta Perry,[*] Rose Whelan,[†] Chi Zhang [‡], and Ryan J. Arsenault[*,1]

[*]*Department of Animal and Food Sciences, University of Delaware, Newark, DE, USA;* [†]*Evonik Operations GmbH, Birmingham, UK; and* [‡]*Center for Bioinformatics and Computational Biology, University of Delaware, Newark, DE, USA*

ABSTRACT Significant changes in growth potential and feed conversion have been bred into the modern broiler chicken for well over 60 yr. These metabolic changes have had significant effects on the immune performance as well. To better understand these genetic differences in immunometabolism we studied the immune response of the modern broiler and the Athens Canadian Random Bred (**ACRB**) heritage broiler strain. We injected newly hatched modern broiler and ACRB chicks intraabdominally with CpG oligonucleotide, an immunostimulatory synthetic oligonucleotide. We conducted species-specific kinome array analysis and gene expression analysis on jejunum and cecal tonsil tissue. We also performed metabolic analysis of blood cells. In the modern birds, there is an initial inflammatory response to the injection at d 3 post-hatch with activation of PI3K-Akt, JAK-STAT, and NF-κB signaling, and IL-1β and IL-6 mRNA expression. By d 15 post-hatch this response changed to deactivation and down-regulation of these immune responses in modern but not heritage broilers. Metabolic analysis showed an increase in glycolysis in peripheral blood mononuclear cells from modern birds given CpG, but no difference in ACRB. These results show that the ACRB birds may have a less inflammatory and more stable immune profile in response to immune stimulation than the modern broilers, possibly resulting in a more disease resistant phenotype overall.

Key words: gut, kinome, broiler, ACRB, CpG

2022 Poultry Science 101:101775
https://doi.org/10.1016/j.psj.2022.101775

INTRODUCTION

Over the last 60 yr, the modern broiler chicken has been continuously selectively bred for rapid rates of growth and muscle deposition (Schmidt et al., 2009), with significant gains made since the 1950s. While the increased growth rate and improved feed conversion ratio of these birds has made the poultry industry one of the most efficient animal production industries, and has provided the world with an inexpensive source of animal protein, these advances have not come without complications. Modern broilers often exhibit skeletal (Julian, 1998) and circulatory/vascular problems (Olkowski, 2007; Abasht et al., 2021), as well as metabolic complications (Jackson and Diamond, 1996; Scheele, 1997) including the metabolic and immune pathology known as woody breast (Kuttappan et al., 2016; Zhang et al., 2021). Perhaps most crucially they often have insufficient or inappropriate immune responses to immune stimulatory challenges (Cheema et al., 2003; Qureshi, 2003). In-feed antimicrobials historically have been used to maintain health and improve growth, but now market demand and government regulations necessitate a shift to antibiotic-free poultry production. In order to keep modern chickens disease-free without antibiotics and to maintain the critical efficiency gains, we have achieved it is important to understand where the immune system may be falling short.

To understand how 60 yr of selective breeding for growth and efficiency have impacted immune responses in modern broilers, it is informative to compare it to the immune system of a chicken that hasn't been selectively bred since the 1950s. The Athens Canadian Random Bred (**ACRB**) bird was originally derived from three broiler strains and one experimental strain of chickens that were used to generate the Ottawa Meat Control Strain (Collins et al., 2016). The strain was then sent to

Received June 4, 2021.
Accepted February 5, 2022.

[1]Corresponding author: rja@udel.edu

the University of Georgia, and they have maintained the population and the breeding program since 1958. The growth parameters have not been selectively altered since, and the ACRB strain is the oldest pedigreed meat-type chicken in existence. As the strain has not been selectively bred since 1957, it is a good side-by-side example to measure how the immunometabolism of the modern broiler has changed and determine the unintended consequences of a breeding focus predominantly based on growth and performance parameters.

In order to study the immune response of modern and ACRB broiler, we administered CpG oligonucleotide (**CpG**), an immunostimulatory treatment that is known to induce immune responses in chickens. The CpG oligonucleotides are synthetic DNA molecules that are a mimic of prokaryotic DNA motifs. Prokaryotic DNA, in contrast to eukaryotic DNA, has a high concentration of cytosine (**C**) and guanine (**G**) nucleotides. Additionally, in prokaryotic DNA these bases are unmethylated, whereas they are mostly methylated in eukaryotic DNA (Bird, 1986; Krieg, 1996). Due to these distinct biochemical properties and the specific pattern in which the C and G bases occur, CpG oligonucleotides are bound and recognized as foreign DNA by pattern recognition receptors (**PRRs**) of the innate immune system (Hemmi et al., 2000; Brownlie et al., 2009), specifically toll-like receptor (**TLR**) 21 in chickens. These oligonucleotides have been used in avian species as an immunostimulatory treatment that leads to increased antibody response when used as an adjuvant (Vleugels et al., 2002). The CpG can also lead to increased heterophil activation, proinflammatory cytokine production, and nitric oxide (**NO**) production when administered in vitro (He et al., 2003). The CpG is protective against *Salmonella enterica* serovar Enteritidis (***S.* Enteritidis**) organ invasion when administered to chicks 24 h prior to challenge with *S.* Enteritidis (He et al., 2005). In this study, we used CpG to induce immune activation in order to study the immune potential of the modern and ACRB broilers.

The intestinal tract is a significant immune organ home to a large population of innate and adaptive immune cells (Wershil and Furuta, 2008), in addition to the site of nutrient absorption. Secondary lymphoid organs in the avian gastrointestinal tract, such as the cecal tonsils, are important sites of germinal center development and lymphocyte maturation. Furthermore, in a production animal optimal gut function is important for rapid growth and efficient utilization of nutrients (Kogut and Arsenault, 2016). In this work, we studied the cecal tonsil and jejunum to consider both the immune and absorptive areas of the poultry gut. We analyzed these tissues by kinomic, gene expression, and metabolic flux analysis. Phosphorylation is a common post-translational modification, especially in immune and metabolic signaling pathways, that can control the activation status of a protein. Observing changes in kinase activity provides information about protein signaling and activation at the most phenotypically relevant molecular level. Coupled with selective gene expression analysis we can determine which signaling pathways are being activated or suppressed, and if expression of key cytokines are affected as a result of the CpG treatment.

In this study, we aim to begin characterizing potential immune changes in the gut of modern broilers due to its aggressive breeding for growth parameters. We used CpG to induce immune activation in order to study the immune changes in the modern and ACRB broilers. Observing changes in kinase activity provides information about protein signaling and activation at the most phenotypically relevant molecular level. Coupled with selective gene expression analysis we determined which signaling pathways were being activated or suppressed, and if expression of key cytokines are affected as a result of the CpG treatment. Our results showed that ACRB birds have a less inflammatory immune profile in response to immune stimulation and a more consistent microbial population and metabolic phenotype than the modern broilers compared to unstimulated birds. Based on kinome and cecal tonsil gene expression data, the modern broilers appear to have a decrease in immune response at d 15 post-hatch.

MATERIALS AND METHODS

Bird Husbandry

Newly fertilized ACRB eggs were acquired from the University of Georgia Poultry Science Department and incubated in Jamesway (Jamesway Incubator Co. Inc., Cambridge, ON, Canada) incubators at 37.5°C and 60% humidity until day of hatch. Embryonic d 16 modern broiler (Ross 308) eggs were acquired from Pedigree Chicks (Beaver Creek, PA) and were incubated in Jamesway incubators at 37.5°C and 60% humidity until day of hatch. At hatch, chicks were removed from incubators and placed onto clean pine shavings on wooden floors in individual colony houses on the University of Delaware farm at approximately 35°C. Each group and strain were placed in randomly assigned, separate 3.35 × 3.96 meter colony house within an initial bird count at hatch of 73 modern birds CpG group, 78 modern birds GpC oligonucleotide (**GpC**) control group, 61 ACRB birds CpG group and 60 ACRB birds in GpC control group. Within 2 wk, once no early mortality was observed, bird numbers were standardized between groups. We do not believe given the house size and bird size at this time the differences in numbers for this period of time had any significant effect on the relative results. At each of 10 collection points 5 birds from each group were removed and sacrificed. Feed and water were provided ad libitum. Corn-soybean based diets were formulated to meet all nutritional needs of the modern broiler (Supplementary Table 1), which contain higher levels of protein, energy. and amino acids than those typically formulated in 1957 (Havenstein et al., 2003). Birds were changed from mash starter feed to a pelleted grower feed on d 12. Birds were changed from grower feed to pelleted withdrawal/finisher feed on d 25. Birds

were observed daily to ensure all were eating and had access to food and water. All animal care and use protocols were approved by the University of Delaware Animal Care and Use Committee (AUP # 86R-2017-0)

Experimental Design

On the day of hatch, chicks were injected intraabdominally (inside the peritoneum) with 0.2 mL of 0.01 M phosphate buffered saline (**PBS**) containing either 25 μg of CpG or 25 μg of the control oligonucleotide GpC, which has been shown not to illicit immune activation in broilers (Ahmad-Nejad et al., 2002). The CpG treated birds were housed separately from the GpC control birds. On d 3, 6, 9, 12, 15, 18, 21, 25, 29, and 34 post-hatch 5 birds from each group were weighed and subsequently sacrificed via cervical dislocation. Tissue samples were collected from the jejunum and cecal tonsils on d 3, 15, and 34. Jejunum was collected from the midpoint between the duodenal loop and the Meckel's diverticulum, both cecal tonsils were collected but only one was used from each bird for kinome or qPCR, sample collection was consistent for all birds and assays. Tissue samples for use in kinome array analyses were snap-frozen in liquid nitrogen and stored at −80°C until further processing. Tissue samples for use in RNA extraction and quantitative real-time polymerase chain reaction (**qRT-PCR**) were placed in 1 mL of RNAlater, stored overnight at 4°C and then transferred to −20°C until further processing.

Kinome Array Analysis

Jejunum and cecal tonsil tissue samples from d 3, 15, and 34 post-hatch were used for kinome array analysis. Processing of each tissue from the groups (2), strains (2), time points (3), and replicates (3) were done on separate, independent peptide arrays to maintain biological replication. Peptide array protocol using PepStar peptide microarrays from JPT Peptide Technologies GmbH (Berlin, Germany) was carried out as described previously (Arsenault et al., 2017) and summarized below with the following modifications. Approximately 40 mg pieces of tissue were cut and homogenized by a Bead Ruptor homogenizer (Omni, Kennesaw, GA) in 100 μL of lysis buffer (20 mM Tris−HCl pH 7.5, 150 mM NaCl, 1 mM ethylenediaminetetraacetic acid (**EDTA**), 1 mM ethylene glycol tetraacetic acid (**EGTA**), 1% Triton X-100, 2.5 mM sodium pyrophosphate, 1 mM Na3VO4, 1 mM NaF, 1 μg/mL leupeptin, 1 g/mL aprotinin, and 1 mM phenylmethylsulphonyl fluoride). All chemicals were purchased from Sigma-Aldrich, Co. (St. Louis, MO) unless specified otherwise. Arrays were then imaged using a Tecan PowerScanner microarray scanner (Tecan Systems, San Jose, CA) at 532 to 560 nm with a 580-nm filter to detect dye fluorescence. The kinome array images were gridded using the GenePix Pro software, and the spot intensity signal was collected as the mean of pixel intensity using local feature background intensity calculation with the scanner saturation level set at 50%.

Peripheral Blood Mononuclear Cell Isolation and Cryopreservation

After sample chickens were killed via cervical dislocation, blood was collected from the neck. The blood was collected in 50 mL conical tubes containing 10 mL of 400 units/mL heparin (Sigma Aldrich) and put on ice. In the lab, the blood samples were poured through sterile gauze into new 50 mL conical tubes. The blood was then centrifuged at 1,400 *g* at 23°C for 20 min with no brake. Plasma was taken off the top of the centrifuged blood samples and pooled, and flash frozen for later use. The buffy coat was then removed from each blood sample and put into a sterile 15-mL conical tube. All replicates from each group were pooled, so the buffy coats from all 5 control birds went into one tube, and the buffy coats from all 5 treatment birds went into another. Enough 0.01M PBS (Sigma Aldrich) was then added to bring the volume in the 15 mL conical to 6 to 8 mL. The suspension was then layered over 4 mL of a 60% Percoll solution (Fisher Scientific, Waltham, MA). This gradient was then centrifuged at 2,000 *g* at 23°C for 20 min with the brake off. The cells were then pulled off the Percoll gradient and washed once with 10 mL of 0.01 M PBS and centrifuged at 300 *g* at 4°C for 10 min. The RBCs were then lysed using 3 lysis steps, where 9 mL of sterile ddH2O was added to the pellet, mixed for 20 s, and then 1 mL of 0.1 M PBS was added to the suspension. The pellet was then centrifuged down, and the lysis step was repeated twice more. The pellet was then washed 3 times with 0.01 M PBS and centrifuged at 300 *g* at 4°C for 10 min. The cells were then counted, and viability was assessed via a trypan blue exclusion assay. The cells were then resuspended in 1 mL of IMDM (Fisher Scientific, Waltham, MA) + 20% fetal bovine serum (**FBS**) (VWR, Radnor, PA) + 10% dimethyl sulfoxide and placed into a Nalgene Mr. Frosty slow chill container (Thermo Scientific) which was then placed into the −80°C freezer.

Seahorse Metabolic Assay

To prepare peripheral blood mononuclear cell (**PBMCs**) that were preserved for use in the Seahorse metabolic assay, cells were thawed in a water bath and then cultured overnight in IMDM + L-glutamine + antibiotic/antimycotic at 37°C in a 95% humidity, 5% CO_2 incubator. After overnight culture, the cells were trypsinized, washed in fresh media and then resuspended in 1 mL of 0.01 M PBS. The cells were then centrifuged down and resuspended in the assay medium, which had been warmed to 37°C (Seahorse Base Medium, Agilent, Santa Clara, CA, 1 mM pyruvate, 2 mM glutamine, 10 mM glucose). The Seahorse plates were coated with Cell Tak (Corning, VWR, Radnor, PA) with a concentration of 22.4 μg/mL for 20 min

Table 1. Real-time quantitative qRT-PCR probes and primers.

RNA target	Probe/primer sequences	Accession number[a]
28S	Probe: 5'-(FAM)-AGGACCGCTACGGACCTCCACCA-(TAMRA)-39 F: 5'-GGCGAAGCCAGAGGAAACT-3' R: 5'-GACGACCGATTGCACGTC-3'	X59733
IL-1β	Probe: 5'-(FAM)-CCACACTGCAGCTGGAGGAAGCC-(TAMRA)-3' F: 5'-GCTCTACATGTCGTGTGTGATGAG-3' R: 5'-TGTCGATGTCCCGCATGA-3'	AJ245728
IL-6	Probe: 5'-(FAM)-AGGAGAAATGCCTGACGAAGCTCTCCA-(TAMRA)-3' F: 5'-GCTCGCCGGCTTCGA-3' R: 5'-GGTAGGTCTGAAAGGCGAACAG-3'	AJ250838
IL-18	Probe: 5'-(FAM)-CCGCGCCTTCAGCAGGGATG-(TAMRA)-3' F: 5'-AGGTGAAATCTGGCAGTGGAAT-3' R: 5'-ACCTGGACGCTGAATGCAA-3'	AJ416937
IFNγ	Probe: 5'-(FAM)-TGGCCAAGCTCCCGATGAACGA-(TAMRA)-3' F: 5'-GTGAAGAAGGTGAAAGATATATCATGGA-3' R: 5'-GCTTTGCGCTGGATTCTCA-32019	Y07922

F = forward; R = reverse; Sequences obtained from Kogut et al., 2003 (Kogut et al., 2003).
[a]Based on genomic DNA sequence.

at room temperature, then washed with 200 μL ddH2O twice. Fifty μL aliquots of either cell suspension or medium alone were placed into the sample wells of a Seahorse Fluxpak plate or the control wells, respectively. A total of 200,000 cells/well from both CpG treated and GpC control modern birds and 600,000 cells/well from both CpG treated and GpC control ACRB birds were used for this assay, as each bird strain yielded different amounts of PBMCs. The plates were then centrifuged at 200 *g* at room temperature for 1 min with no brake. The plate with the cells was then incubated at 37°C for 25 to 30 min in a non-CO_2 incubator. After the non-CO_2 incubation, an additional 130 μL of media was added to each well, and the plate was placed in the Seahorse XFp analyzer (Agilent) and run on a blank template for 28 cycles and oxygen consumption rate and extracellular acidification data were collected.

RNA Extraction and qRT-PCR

RNA was isolated from the tissue samples (approximately 20 mg of tissue) using the Qiagen RNeasy Mini-Kit, following the "Purification of Total RNA from Animal Tissues" protocol provided in the RNeasy mini handbook. The tissues were lysed in a 2 mL vial with 1.4-mm ceramic beads with 600 μL of buffer RLT in a Bead Ruptor 24 run on setting 6 for two cycles of 10 s. The rest of the steps in the protocol were followed, and the isolated RNA was eluted into ultrapure water, and stored at −80°C until further analysis. RNA quality was verified by quantification on a NanoDrop 1000 Spectrophotometer (Thermo Scientific) and gel electrophoresis of the RNA samples on an Invitrogen E-Gel EX 1% Agarose (Invitrogen, Carlsbad, CA). The RNA was used with the Applied Biosystems TaqMan RNA-to-CT 1-Step kit following the protocol provided. The primers and probes for the housekeeping gene and cytokines of interest were ordered from Integrated DNA Technologies (Coralville, IA; Table 1). The qRT-PCR was performed on an Applied Biosystems 7900HT Real Time PCR System with a standard 96-well block. Each sample was run in triplicate.

Statistical Analyses

The modern broiler weights were measured as a group between d 3 and 12 post-hatch and then individually between d 15 and 34 post hatch. When the weights were taken individually, a two-tailed Student's *t*test was used to compare the weights between the treatment and control birds and determine significant difference, and a *P*-value of < 0.05 was considered significant. The ACRB birds were only weighed individually on d 29 and 34 post-hatch, at all other time points they were weighed as a group. When the ACRB birds were weighed individually, a two-tailed Student's *t*test was again used to compare weights between treatment and control birds.

The kinome fluorescent signal output data files were analyzed using the PIIKA2 peptide array analysis software (http://saphire.usask.ca/saphire/piika/index.html) (Trost et al., 2013). The resulting data points were normalized to eliminate variance due to technical variation such as random variation in staining intensity between arrays or between blocks within an array. Variance stabilization normalization was performed. There were 3 biological replicates for each sample and sample was run on its own independent peptide array, and the normalized fluorescence data for the 3 replicates were averaged together. Within each array there were 9 technical replicates of each peptide. PIIKA2 then performed one-tailed *t* tests to determine the statistical significance of the change in phosphorylation at each peptide fragment between the treatment and the control tissues, generating a fold change and a *P*-value. Peptides with fold changes with a *P*-value < 0.05 were considered statistically significantly differentially phosphorylated between treatment birds' samples and control. In the rest of the manuscript the word "significant" when used in reference to kinome data will refer to these statistically significantly differentially phosphorylated peptides. Significant peptides/protein data was input into the

protein-protein interaction database STRING (Szklarczyk et al., 2015) for interaction analysis and KEGG pathway analysis (Kanehisa et al., 2017).

For the qRT-PCR data analyses the raw CT values from the qRT-PCR were used in a ΔΔCT calculation to determine fold change of mRNA expression between treatment and control tissue samples. Determination of significant differences in the fold changes for individual genes between time points determined by ANOVA followed by Bonferroni-corrected *P*-values (* = $P < 0.05$, ** = $P < 0.01$).

RESULTS

Growth Rates

The modern broilers given the CpG injection weighed significantly less than the modern broilers injected with the control GpC on d 18, 21, and 29 post-hatch. Bird weights from d 0 to d 12 post-hatch were not collected separately for each modern bird. Bird weights were not collected separately from d 0 to d 25 for each ACRB bird, thus statistical analysis was not possible on these days. At the end of the experimental period, the average weight of the modern birds was 2.5 kg. The ACRB birds had an final average weight of 0.45 kg (Figure 1).

Kinome and Signaling Pathway Analysis

In order to visualize the phosphorylation differences between the modern and ACRB birds following CpG injection we compared the differences in differentially phosphorylated proteins (CpG treatment vs. GpC control groups within strains). These time-matched comparisons are shown in Venn diagrams in Figure 2. As seen in Figure 2, in the cecal tonsil the majority of the proteins differentially phosphorylated postchallenge overlap between the 2 strains. However, at d 15 there is less overlap, the phosphorylation changes in response to CpG injection are similar between the bird strains in only 51.1% of proteins. A similar trend was observed in the jejunum but the least overlap occurred at d 34 with 55.6% of proteins overlapping between the strains.

As there were a large number of unique protein phosphorylation changes for each bird strain, especially at d 15 in the cecal tonsil and d 34 in the jejunum (Figure 2), we input these unique proteins from each strain into STRING (Szklarczyk et al., 2015) and a list of Kyoto Encylopedia of Genes and Genomes (**KEGG**) pathways was generated. The top 20 pathways listed were compared, unique pathways from each list (i.e., were not present in the other strain's data) are shown in Tables 2 and 3 for the modern and ACRB broilers, respectively. In the modern birds, there are several immune related pathways that are uniquely affected by CpG at d 3 and d 34 in both the cecal tonsils and jejunum (Table 2). Note that the pathway tables list a number of specific diseases, this is an indication that phosphorylation of signaling proteins related to disease immune responses were altered, not that the birds are infected with those diseases. At d 15, only a single pathway was unique for both cecal tonsil and jejunum in the modern birds (Table 2). In the ACRB birds, there was a mix of unique

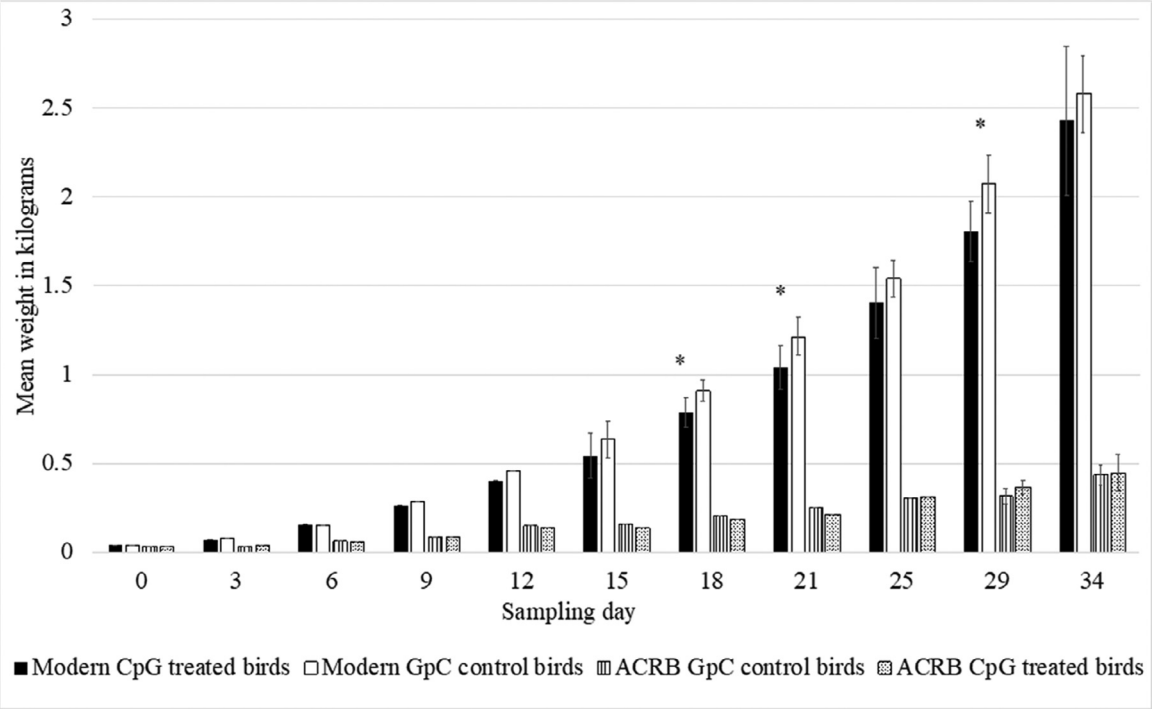

Figure 1. The average weights of both ACRB and modern birds at each sampling time point during the trial (n = 5). Only treatment-control pairs within a strain were compared for statistical significance. * refers to *P*-value < 0.05. Each bar from d 15−34 for modern birds and d 29−34 for ACRB birds represents n = 5, on d 0−12 modern birds and d 0−25 ACRB birds were weighed as groups. Birds were injected with CpG on day of hatch. Abbreviation: ACRB, Athens Canadian Random Bred.

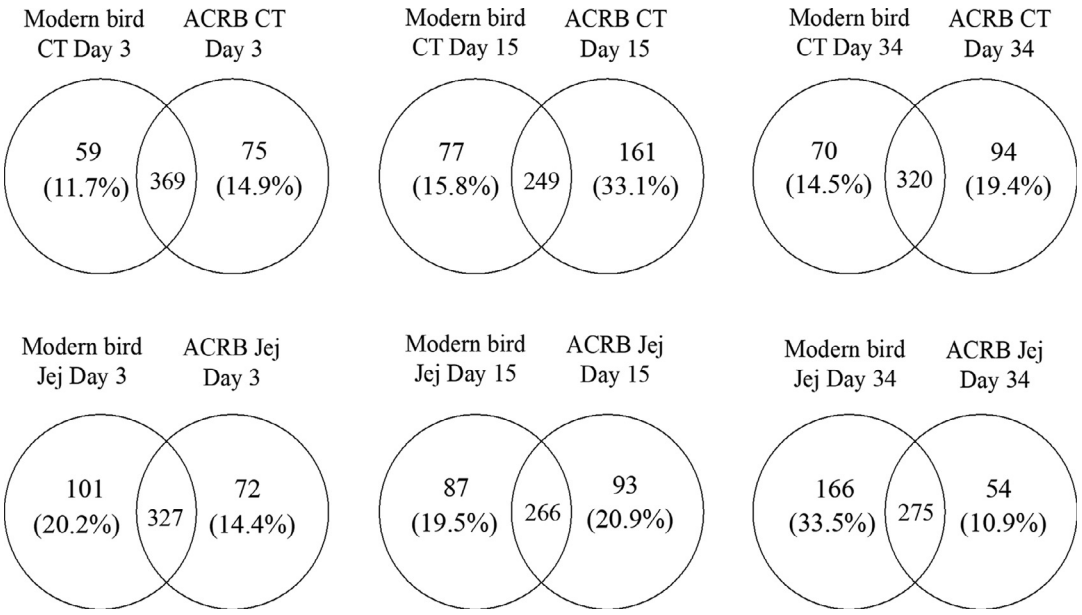

Figure 2. Comparison of unique and shared significant proteins between the modern broiler and ACRB broiler tissue samples. Significant proteins displayed a representative *P*-value of ≤ 0.05, n = 3 tissues per group and timepoint, following variance normalization and *t* test. Protein Uniprot IDs were compared and separated into unique or overlapping groups. CT refers to cecal tonsils, Jej refers to jejunum. Birds were injected with CpG on day of hatch. Abbreviation: ACRB, Athens Canadian Random Bred.

Table 2. KEGG pathways unique to the modern broiler compared to ACRB.

Cecal tonsil			Jejunum		
D 3	D 15	D 34	D 3	D 15	D 34
Fc epsilon RI signaling pathway	Toxoplasmosis	Fc gamma R-mediated phagocytosis	Adipocytokine signaling pathway	Fc gamma R-mediated phagocytosis	Adipocytokine signaling pathway
Fc gamma R-mediated phagocytosis		Insulin signaling pathway	AMPK signaling pathway		Influenza A
MAPK signaling pathway		Natural killer cell mediated cytotoxicity	HIF-1 signaling pathway		Measles
		TNF signaling pathway	MAPK signaling pathway		
			Viral carcinogenesis		

STRING output KEGG pathways.
Input data were proteins uniquely differentially phosphorylated as compared to the other bird strain.

immune and metabolic pathways that were altered at at d 3, 15, and 34 (Table 3).

To better understand why the changes in phosphorylation in the cecal tonsil of the modern broiler at d 15 stand out compared to the other 2 time points, we compared the full significant protein lists between ACRB and modern broiler at d 15. The direction of the change in phosphorylation (increased or decreased relative to control) was not considered for this analysis, but only significance. When the 77 proteins unique to the modern broiler d 15 cecal tonsil were subjected to pathway enrichment analysis results included Phosphoinositide 3-kinase - RAC-alpha serine/threonine-protein kinase (**PI3K-Akt**) pathway, a major immunometabolic pathway, as well as the Rap1 and Ras signaling pathway, which are involved in interferon gamma (**IFNγ**) signaling and cell survival signaling respectively (Table 4). When the 249 proteins shared between the modern broilers' d 15 cecal tonsil and the ACRB d 15 cecal tonsil were subjected to pathway analyses the significantly enriched signaling pathways included major immunometabolic signaling pathways, such as the mitogen-activated protein kinase (**MAPK**) signaling pathway, PI3K-Akt signaling, and the insulin signaling pathway (Table 4). In the set of significant proteins that were unique to the ACRB d 15 cecal tonsil, there were more immune response related pathways that were among the top 5 significantly enriched KEGG pathways, in addition to immunometabolic signaling pathways (Table 4).

PI3K-Akt signaling pathway was significantly enriched in the set of proteins unique to the modern broiler d 15 cecal tonsil, and in the shared set of proteins between both strains. The reason this pathway appeared in the list of top pathways despite the protein lists being unique was that different protein members that make up the pathway were phosphorylated in each strain. This result prompted further investigation of the phosphorylation status of the peptides involved in this pathway on d 15 in both the modern broiler and ACRB cecal tonsil tissue samples. The PI3K-AKT pathway activation status associated with the phosphorylation site changes in

Table 3. KEGG pathways unique to the ACRB compared to modern broiler.

Cecal tonsil			Jejunum		
D 3	D 15	D 34	D 3	D 15	D 34
Bacterial invasion of epithelial cells	Epstein-Barr virus infection	Adipocytokine signaling pathway	Bacterial invasion of epithelial cells	Adipocytokine signaling pathway	Fc epsilon RI signaling pathway
Endocytosis	FoxO signaling pathway	AMPK signaling pathway	Chemokine signaling pathway	Epstein-Barr virus infection	Fc gamma R-mediated phagocytosis
Leukocyte transendothelial migration	Hepatitis C	Chemokine signaling pathway	Endocytosis	FoxO signaling pathway	Hepatitis C
	Neurotrophin signaling pathway	Endocytosis	Leukocyte transendothelial migration	Glycolysis / Gluconeogenesis	HIF-1 signaling pathway
		Fatty acid metabolism		NF-kappa B signaling pathway	Tuberculosis
		HTLV-I infection		TNF signaling pathway	
		PI3K-Akt signaling pathway		Toll-like receptor signaling pathway	
		Viral carcinogenesis			

STRING output KEGG pathways.
Input data were proteins uniquely differentially phosphorylated as compared to the other bird strain.

the CpG challenged versus control animals are shown in Table 5 for both the modern and ACRB strains. In the modern broiler d 15 cecal tonsil, there was deactivation of signaling through the pathway. 5′ adenosine monophosphate-activated protein kinase (**AMPK**) was also deactivated in the modern broiler d 15 cecal tonsils. In the ACRB d 15 cecal tonsil, conversely, there was activation of signaling through the PI3K-Akt pathway, while mechanistic target of rapamycin (**mTOR**) was deactivated. AMPK was phosphorylated significantly in ACRB d 15 cecal tonsils, but not at an activation site. Nuclear factor kappa-light-chain-enhancer of activated B cells (**NF-κB**) was also active in the ACRB d 15 cecal tonsil, and not in the modern broiler d 15 cecal tonsils (Table 5).

As both the TLR signaling pathway (Supplementary Table 2) and T cell receptor signaling pathway (Supplementary Table 3) were significantly enriched when considering the unique to ACRB d 15 cecal tonsils significant proteins (Table 4), the signaling activity through both of these pathways was further examined. The Toll/interleukin-1 receptor domain-containing adapter protein (**TIRAP**) was significantly phosphorylated and activated in the ACRB d 15 cecal tonsils, and not in the modern broilers' d 15 cecal tonsils (Table 5). Mitogen-activated protein kinase 8 (**JNK1**) was significantly phosphorylated and thus significantly activated in both the modern broilers' and ACRB d 15 cecal tonsils (Table 5). Phosphatidylinositol-4,5-bisphosphate 3-kinase catalytic subunit delta isoform (**PIK3CD**) was significantly phosphorylated at an inhibitory target site in the ACRB d 15 cecal tonsils, and not in the modern broilers' d 15 cecal tonsils (Table 5). In the ACRB d 15 cecal tonsils the transcription factor Activator protein 1 (**AP-1 or Jun**) was significantly phosphorylated on the 2 phosphorylation target sites included on the array, but this transcription factor was significantly dephosphorylated on one of the target sites in the modern broilers' d 15 cecal tonsils (Table 5).

Table 4. KEGG pathways generated from significant protein lists.

KEGG pathways[1]			
Unique to modern broiler	Pathway ID	Count	FDR
PI3K-Akt signaling pathway	hsa04151	6	0.00014
Pathways in cancer	hsa05200	7	0.00014
Hepatitis B	hsa05161	4	0.00083
Rap1 signaling pathway	hsa04015	4	0.0024
Ras signaling pathway	hsa04014	4	0.003
Unique to ACRB	pathway ID	count	FDR
MAPK signaling pathway	hsa04010	22	7.76E-13
T cell receptor signaling pathway	hsa04660	15	1.1E-12
Osteoclast differentiation	hsa04380	15	1.46E-11
Toll-like receptor signaling pathway	hsa04620	13	2.59E-10
AMPK signaling pathway	hsa04152	13	1.34E-09
Shared by modern broiler and ACRB	pathway ID	count	FDR
Pathways in cancer	hsa05200	55	1.53E-31
PI3K-Akt signaling pathway	hsa04151	46	6.91E-30
MAPK signaling pathway	hsa04010	42	1.47E-28
Insulin signaling pathway	hsa04910	31	2.25E-26
Central carbon metabolism in cancer	hsa05230	24	2.16E-24

[1]Top five enriched STRING output KEGG pathways in the set of significant peptides from cecal tonsil samples at day 15. Pathway ID is KEGG identifier, count is proteins in dataset in pathway, FDR is false discovery rate.

In the T-cell receptor signaling pathway there were phosphorylation events leading to T cell activation in the ACRB birds' d 15 cecal tonsils. Src family tyrosine kinase (**FYN**) and Zeta-chain-associated protein kinase 70 (**ZAP70**) are phosphorylated on residues that would lead to downstream T cell activation. Interleukin-2-inducible T-cell kinase (**ITK**), however, was not phosphorylated on its activation site (Table 5). Nuclear factor of activated T-cells, cytoplasmic 1 (**NFAT2**) was dephosphorylated significantly at 2 priming residues, and not significantly altered at the third in the ACRB birds' cecal tonsils. In the modern broiler d 15 cecal tonsils, NFAT2 was also significantly dephosphorylated on the 2 "priming" sites, however it was significantly phosphorylated on a third site in between the two priming sites.

The Metabolic Flux Data Support the Bird Strain Differences in Signaling on D 15

PBMCs isolated from the modern broilers that received the CpG treatment showed different oxygen

Table 5. Summary table of key signaling differences in the modern broilers' d 15 cecal tonsil and the ACRB birds' d 15 cecal tonsil.

Proteins	Modern broiler d 15 cecal tonsils phosphorylation at each site[1]	Activation status[2]	ACRB d 15 cecal tonsils phosphorylation at each site[1]	Activation status[2]
4E-BP1	- - -	-	↓ ↓ -	Active
AKT1	↓ -	Inactive	↑ -	Active
AMPK subunit alpha 1	- ↓ ↓	Mixed effects	↑ - -	Inactive
APMK subunit alpha 2	↑	No activity affiliated	-	No activity affiliated
ERK2	-	-	↑	Active
FYN	- -	-	↑↓	Inactive
GRB2	↑	Inhibition of signaling	-	-
GSK3B	↑ ↑ -	Active	- ↑ ↓	Mixed effects
ITK	-	-	↓	Inactive
JNK1	↑	Active	↑	Active
Jun	- ↓	Inactive	↑ ↑	Active
mTOR	- - -	-	↓ ↓ -	Inactive
NFAT1	-	-	↑	No activity affiliated
NFAT2	↓ ↑ ↓	Mixed effects	↓ - ↓	Active
NFKB1	- -	-	↑ ↑	Active
PIK3CD	-	-	↑	Inhibited
p70S6K	- ↑ ↑	Active	↓ ↓ ↓	Inactive
SOS1	- -	-	↓ -	Inactive
TIRAP	-	-	↑	Active
TSC2	↑ - -	Inhibited	↓ ↓ -	Active
ZAP70	↓ -	Inactive	- ↑	Active

[1]Most proteins are presented on the peptide array by multiple peptide kinase target sequences. The arrows and dashes represent the statistically significant changes in phosphorylation at each target site between the treatment and control birds. An up arrow indicates significantly increased phosphorylation. A down arrow indicates significantly decreased phosphorylation. A dash indicates no significant difference in phosphorylation between the treatment and control birds.

[2]Activation status refers to effect on protein of given phosphorylation event. Function annotation was determined using the PhosphositePlus online database (Hornbeck et al., 2015). Active indicates a protein function activating phosphorylation event, inactive indicates the protein function is not active, inhibited indicates the protein activity is being actively suppressed, mixed effects indicates that the phosphorylation events both activate and inhibit certain functions of the protein, no activity affiliated indicates that the phosphorylation site does not presently have an annotated functional effect.

consumption rates (**OCR**) and extracellular acidification rates (**ECAR**) when compared to the PBMCs from control birds on d 15 post-hatch. Conversely, the PBMCs isolated from the ACRBs did not show different rates of ECAR and OCR between the treatment and control birds on d 15 post-hatch (Figure 3).

The qRT-PCR Data Support the Signaling Patterns Seen in the Kinome Array Data

To confirm the patterns in immunometabolic signaling seen in the kinome data, qRT-PCR was performed. The 28s gene was used as the housekeeping gene, and the expression of interleukin (**IL**)-1β, IL-6, IFNγ, and IL-18 was examined in each of the treatment birds compared to the control birds (Figure 4). All fold changes described below showed significant change compared to control unless indicated. In the modern broiler d 3 cecal tonsils, IL-1β and IL-6 showed an 8.3- and 5.4-fold increase respectively in the treatment birds compared to the control birds. IL-18 and IFNγ also showed fold increases in the modern broiler d 3 treatment birds' cecal tonsils compared to control, though these fold increases were more modest (2.3 and 1.7 respectively). Interestingly, on d 15 in the modern CpG treatment birds' cecal

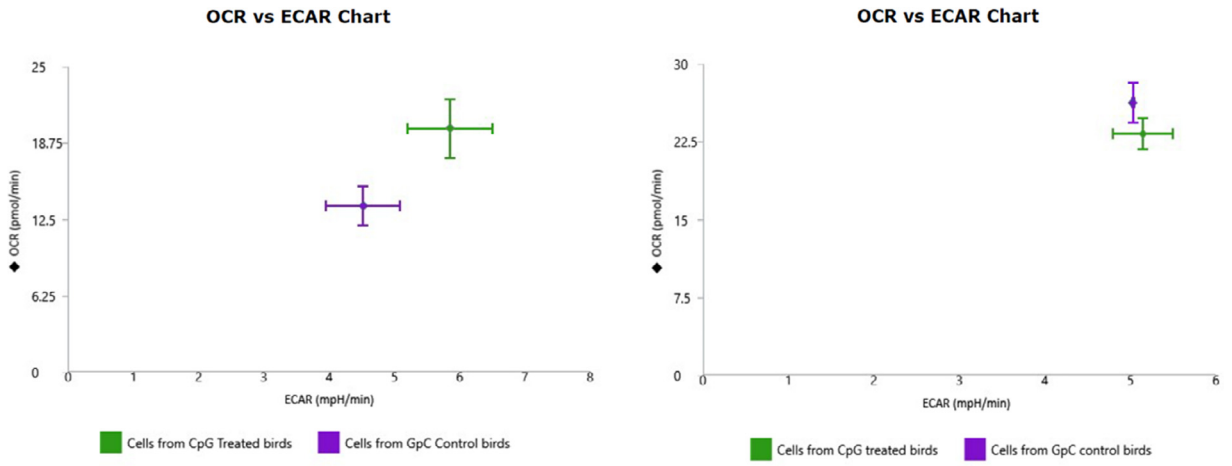

Figure 3. The metabolic activities of peripheral blood mononuclear cells (PBMCs). PBMCs were isolated from treatment and control modern broilers and treatment and control ACRB birds and were assessed using a Seahorse XFp Analyzer. (Left) For modern broilers, the two treatments separated based on both ECAR and OCR values (x and y axes). (Right) For ACRB broilers, the two treatments did not separate based on ECAR or OCR. Abbreviations: ACRB, Athens Canadian Random Bred; ECAR, extracellular acidification rates; OCR, oxygen consumption rates.

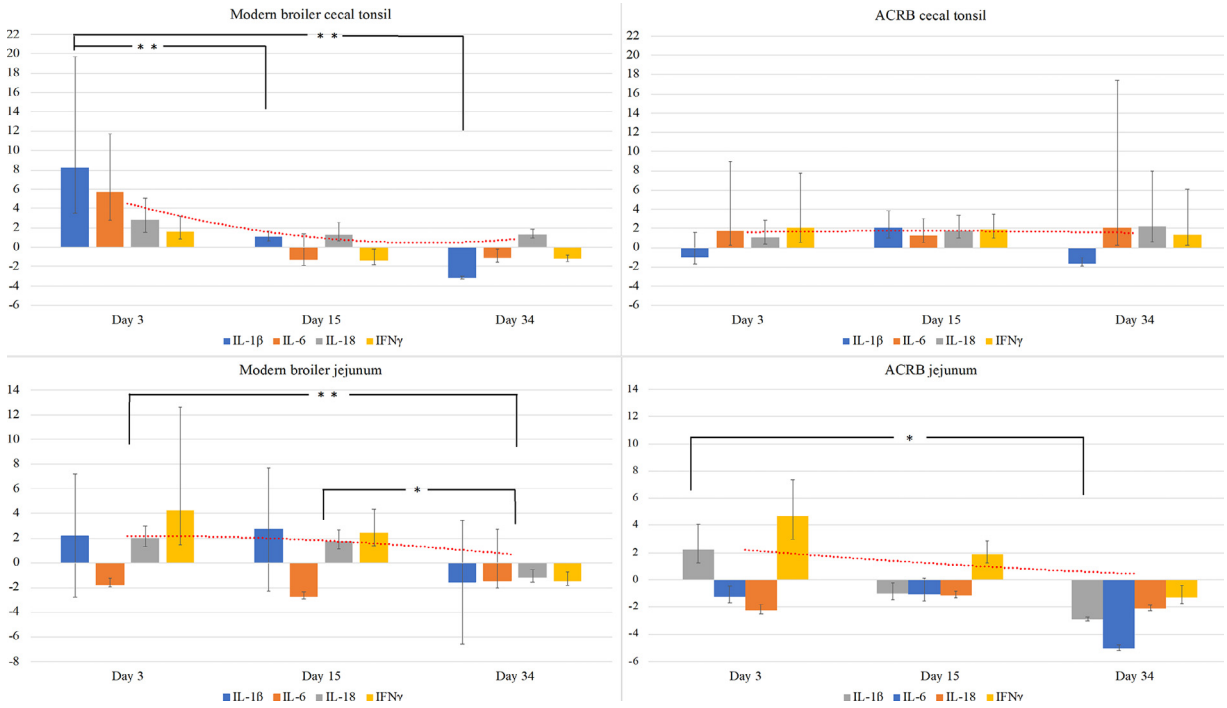

Figure 4. qRT-PCR mRNA expression of key cytokines. For fold-change calculations raw C_T values were used for a $2^{-\text{deltadeltaC}}{}_T$ calculation to determine the fold change in expression of each cytokine in the treatment birds' tissue samples compared to control. To show the trends in gene expression the average expression fold change for all four genes on each day were averaged together and a polynomial trend line was generated based on these average values. Differences between days was determined by ANOVA with Bonferroni-corrected *P*-values (* = $P < 0.05$, ** = $P < 0.01$).

tonsils IL-6 and IFNγ actually showed a fold-decrease in comparison to the control birds (1.43- and 1.25-fold decrease respectively). IL-1β and IL-18 still had higher expression in the treatment birds' cecal tonsils than the control birds, although the fold increase of IL-1β expression was much lower than the increase seen on d 3. On d 34 in the modern broiler treatment birds' cecal tonsils control the IL-18 expression was approximately equal compared to the control birds (1.3-fold increase) but the expression of all the other cytokines was decreased in the treatment birds compared to control.

In the modern broiler's jejunum samples, there was increased IL-1β and IL-18 expression in the treatment birds compared to the control birds on d 3, but the fold increases were modest compared to those seen in the cecal tonsils (2.2 and 2.0, respectively, not signficant). On d 3 the IFNγ expression showed the largest fold increase between the treatment birds and control birds (4.3). Interestingly, IL-6 expression was actually decreased in the jejunum of the modern broiler treatment birds on d 3 compared to the control birds (3.33-fold decrease). On d 15 in the modern broiler jejunum there was increased expression of IL-18 and IFNγ. The IL-6 expression was still lower in the jejunum of the treated birds than in the control birds' jejunum. On d 34 in the modern broiler's jejunum the expression of IL-18 and IFNγ were lower in the treatment birds' tissues than the control birds.

In the ACRB birds' cecal tonsils all of the cytokines showed elevated expression in the treatment birds compared to the control birds, with the exception of IL-1β on d 3 (not significant) and 34. The fold-increase for all other cytokines was between 1 and 2.3. In the ACRB birds' jejunum there was a fold-increase in expression of IL-1β and IFNγ on d 3, while the other 2 cytokines actually showed lower expression in the treatment birds than in the control birds' jejunum. The expression of IFNγ remained elevated in the treatment birds' jejunum compared to the control birds on d 15. By d 34, expression of all four cytokines was lower in the treatment birds than in the control birds.

DISCUSSION

In this study, we injected newly hatched modern broiler and ACRB chicks intra-abdominally with either the immunostimulatory synthetic oligonucleotide CpG or a control nonstimulatory nucleotide GpC. The CpG injection affected the growth of the modern broiler but did not have a significant impact on the ACRB birds' growth. Generating an immune response to a pathogen is an energetically costly enterprise, and this could contribute to the apparent decrease in growth seen in the modern broiler when the immune system was stimulated (Klasing et al., 1987; Klasing, 2007). The qRT-PCR data support this observation, as seen in the fold-increase of expression of key inflammatory cytokines in both the modern broiler's jejunum and cecal tonsils on d 3. However, the significant differences in weight are not apparent until d 18, once weight measurements were taken on individual birds and differences were statistically discernable. The ACRB birds' growth, conversely, was not significantly impacted by the CpG injection at these later time points. As the ACRB birds have not been intensively selectively bred, they may maintain

more metabolic "flexibility" in terms of even resource allocation between growth and immunity, switching to response upon stimulation and then returning to homeostasis and growth. Though here we only used a single immune stimulate which targets a specific part of the innate immune system, these results suggests a bird that is better able to cope with stressors, as was seen when the effects of heat stress on ACRB birds and modern broilers are observed (Berrong and Washburn, 1998).

The CpG treatment exerted a more divergent effect on the birds' cecal tonsil between strains than the jejunum at d 15 (Figure 2). Pathway analysis of the kinome data at d 15 in the cecal tonsil showed a limited immune response unique to the modern birds (Table 2). Day 15 post hatch is a vulnerable time point for modern broiler, as this is when disease challenges such as necrotic enteritis begin to manifest (Helmboldt and Bryant, 1971; Cooper et al., 2013). This is also the time point when the rate of breast muscle deposition in modern birds continues to increase relative to other organs, whereas this deposition plateaus at this point in a heritage bird (Schmidt et al., 2009).

Possibly the cecal tonsil was more directly impacted than the jejunum because the cecal tonsil is home to a concentrated population of lymphocytes (Moral et al., 1998). By d 15 post-hatch, germinal centers appear in the cecal tonsil and the B-cell population increases from there with age (Oláh et al., 2014). It is likely that lymphocyte populations in the cecal tonsil are responsible for more of the divergent immune-related signaling changes seen in the cecal tonsil tissue samples. In the ACRB birds' cecal tonsil on d 15, there was increased signaling activity through the PI3K-Akt pathway and the T cell receptor signaling pathway (Table 4). The PI3K-Akt pathway is a key immunometabolic pathway, and the interactions between this pathway and the mTOR signaling pathway can determine the fate of an immune cell, such as a T lymphocyte. Simultaneous activation through the PI3K-Akt pathway, deactivation of mTOR, and activation of AMPK together leads to the development of regulatory T cells (Michalek et al., 2011; Gerriets and Rathmell, 2012), which was an activation pattern observed in response to CpG stimulation in the ACRB d 15 cecal tonsil. Akt was phosphorylated on one of its activation sites (Table 5) while, mTOR was significantly dephosphorylated on its activation sites. Additionally, the downstream phosphorylation targets of mTOR, Ribosomal protein S6 kinase beta-1 (**p70S6K**) and eukaryotic translation initiation factor 4E-binding protein 1 (**4E-BP1**) were also significantly dephosphorylated in the ACRB d 15 cecal tonsil. Finally, AMPK was significantly phosphorylated, as was its downstream target Acetyl-CoA carboxylase in these birds, although these phosphorylation sites do not have a functional annotation at this time. The data suggests a mixed immunological response in the ACRB birds cecal tonsil at d 15; the T cell receptor signaling pathway activation is suggestive of a T lymphocyte response, but the metabolic data (mTOR deactivation) suggest a regulatory T lymphocyte. This may suggest the tissue is primed for response but not actively producing immune effector proteins. These results also suggest the bird is developing mechanisms to mediate inflammation and maintain homeostasis.

There was also activation through the TLR signaling pathway in the ACRB birds' d 15 cecal tonsil. The transcription factor AP-1, which is a dimeric protein composed of Jun and Fos, has been shown to work in concert with NFAT to influence gene transcription in cells (Macián et al., 2001). AP-1 was activated downstream of Ras and extracellular signal−regulated kinases (**ERK**) / c-Jun N-terminal kinases (**JNK**) signaling, which are components of the TLR signaling pathway (Kawai and Akira, 2006; Turpaev, 2006). The activity of the transcription factor NFAT is controlled by a gradient of phosphorylation at different target sites, and its phosphorylation at these different sites is controlled by kinases such as JNK and glycogen synthase kinase (**GSK3**) (Hogan et al., 2003). In the ACRB birds' day 15 cecal tonsil there was activation of signaling through this pathway, and this culminates in activation of Jun at key phosphorylation target sites (Table 5). It is, therefore, possible that the transcription factors NFAT and AP-1 are working together in the treated ACRB d 15 cecal tonsil to modulate immune cell responses. AP-1 controls a number of cellular processes including differentiation, proliferation, and apoptosis while NFAT induces expression of several immune genes.

In the modern broiler d 15 cecal tonsil, growth factor receptor-bound protein 2 (**GRB2**) was phosphorylated at an inhibitory site (Table 5). This blocks the association of GRB2 with son of sevenless (**SOS1**) to which subsequently blocks Ras and MAPK signaling (Li et al., 2001). This signaling pathway has a role in insulin signaling, growth factor receptor signaling, and PI3K-Akt signaling and can also be activated by cytokine signaling, as well as downstream of B and T cell receptor signaling. This shows a functional immune response in the ACRB birds, while this pathway doesn't appear to be active in the modern broiler's d 15 cecal tonsil. The transcription factors that are activated in the ACRB d 15 cecal tonsil (NF-κB, Jun) are not active in the modern broiler's cecal tonsil, further highlighting a signaling shut down in this tissue.

Interestingly, mTOR signaling was active in the modern birds as indicated by the phosphorylation of a downstream target of mTOR activity p70S6K. The tuberin sclerosis 2 (**TSC2**) protein was also phosphorylated significantly in the modern broiler cecal tonsil from d 15, inactivating it's functionality as an inhibitor of mTOR signaling (Inoki et al., 2002, p. 2). However, despite some activation along the mTOR pathway, 4E-BP1 was not significantly phosphorylated, and its phosphorylation and subsequent disassociation from eukaryotic Translation Initiation Factor 4E (**eIF4E**) is necessary for the initiation of translation. Activation of mTOR signaling has also been shown to be inhibitory of the PI3K-Akt signaling pathway, so this may explain decreased signaling along PI3K-Akt in the modern broiler d 15 cecal tonsil (Tremblay and Marette, 2001;

Harrington et al., 2005). PI3K-Akt signaling is deactivated in "growth factor withdrawal", which is in agreement with the inhibition of signaling seen through GRB2 and is suggestive that there was a lack of growth factor signaling to these cells (Zhang et al., 2006, p. 1). It could be that the metabolic demands of muscle growth in these birds at this time point mean that the energetic demands of the immune system are neglected or are not receiving growth/differentiation signals at all.

The direction of metabolic activities of an immune cell can determine its fate and inflammatory status (Rodríguez-Prados et al., 2010; Chang et al., 2013; O'Neill and Hardie, 2013). Increased OCR is indicative of oxidative phosphorylation, and increased ECAR is indicative of glycolysis. Immune cell fate is partially determined by cell metabolism; effector T cells exhibit higher rates of glycolysis and depend on glucose uptake. Regulatory T cells instead rely primarily on fatty acid oxidation for energy and inhibit glycolytic processes (Michalek et al., 2011). The PBMCs isolated from modern broilers that were given the CpG treatment demonstrated higher rates of both OCR and ECAR, which suggests that the cells were more metabolically active compared to PBMCs from the control birds. Conversely, in the ACRB birds one cannot distinguish between the treatment and control birds' PBMCs based on OCR and ECAR. The Seahorse data may indicate that the ACRB birds' PBMCs are not impacted by the immunostimulatory injection, and the response to the injection was localized to the gut tissues and not systemic in these birds, or the CpG did not result in additional "priming" of PBMCs as they were already strongly metabolically active in these birds. What the impact of these metabolic changes on PBMC fate and function is remains to be determined.

The qRT-PCR data also support the idea that the immune system is not optimally functional during periods of high growth in the modern birds. Initially on d 3 after the CpG injection there was a large fold-increase in mRNA expression of potent inflammatory cytokines in the modern broiler's cecal tonsil as well as the jejunum to a lesser extent. There was also activation of cell signaling seen in the kinome data, such as Janus kinase-signal transducer and activator of transcription (**JAK-STAT**), tumor necrosis factor (**TNF**)-receptor associated factor 2 activation, mTOR signaling, and phosphorylation of Caspase-1. There was also some indication of NF-κB activity, although the proteolytic cascade leading to its activation does not appear to be completely activated. All these signaling events would either contribute to or be downstream of the synthesis of proinflammatory cytokines such as IFNγ and IL-1β. CpG drives Th1-type immune responses, and this may be demonstrated by the increase in IFNγ expression seen in the cecal tonsil and jejunum (Zimmermann et al., 1998). By d 15, however, the signaling activity in the modern broilers' cecal tonsil has dropped off as seen in the kinome data, and there was decreased mRNA expression of proinflammatory cytokines. In the ACRB birds, there was activation of Nf-κB on d 3 post-hatch as well as signaling activation through the PI3K-Akt pathway, and this continued through to d 15.

It is interesting that the increase in IL-6 expression in both the modern broiler and ACRB treatment birds was limited to the cecal tonsil. It has been shown that IL-6 can negatively influence barrier function in the intestinal epithelial cells, so expression of this interleukin may be limited in the jejunum to preserve the barrier integrity (Suzuki et al., 2011). It is also interesting to note that the depression of cytokine expression on d 15 in the modern broiler was limited to the cecal tonsil, and this depression was not seen to the same extent in the jejunum. This decrease in expression of proinflammatory cytokine mRNA occurs in tandem with the decrease in signaling through key activation pathways in the modern birds' d 15 cecal tonsil such as the JAK-STAT pathway and PI3K-Akt pathway. This larger negative impact on cecal tonsil tissues could also be due to prioritization of energy and nutrients for function of the intestinal tissues as a result of breeding for efficient feed conversion, rather than growth and development of immune cells.

In conclusion, these data indicate that the heritage birds exhibit a more constant immune response to early injection with CpG, whereas in the modern birds this response was dynamic as the birds' age. Initially, in the modern broilers there was robust activation through immunometabolic signaling pathways and increases in the mRNA expression of key inflammatory cytokines in both the jejunum and the cecal tonsil. However, at d 15 post-hatch this response seemingly drops off and there was deactivation through immunometabolic signaling pathways. In the ACRB birds, conversely, the level and direction of signaling activity in both the jejunum and the cecal tonsil remains fairly constant, as does the increase in proinflammatory cytokine mRNA. The immune status of modern broilers at approximately 2 wk post-hatch bears further investigation, as this is a critical age for the birds. While the direct response of the birds to the CpG stimulation would have been well past at d 34, or even 15, immunometabolic consequences of early life events can perpetuate. It is possible that this early and direct stimulation of the immune system altered the immunometabolic programing of these birds over the course of their growout.

With the critical need to increase worldwide food production and enhance global food security, while at the same time improving animal health and welfare (Henchion et al., 2017), a simple return to heritage genetics and slow growing chicken is inappropriate. We may be reaching the limit of genetic growth potential and future work with diet formulations and immune modulating therapies, as well as further clarification of microbiome's role in immune response development, could potentially modulate the immune response of the modern broiler to effectively prime the immune system for response and allow modern broilers to resist a variety of environmental stressors and pathogens. Intervention programs as specific times of grow out, such as the 15 d

described here, may also help improve resistance to disease, at the same time, maintaining the significant efficiency gains achieved in the past 60 yr.

ACKNOWLEDGMENTS

This research was funded by Evonik Nutrition and Care, GmbH. The authors acknowledge The Department of Poultry Science, University of Georgia for the ACRB eggs. Pedigree Chicks, Beaver Creek, PA for the modern broiler eggs.

Role of the funding source: R.W. is an employee of Evonik Nutrition and Care. R.W. took part in the conceptualization of the protocol and editing of the manuscript. The funder and employees of funder had no role in the collection, analyses, or interpretation of data; in the writing of the manuscript, or in the decision to publish the results.

DISCLOSURES

The authors have no conflicts of interest to report.

SUPPLEMENTARY MATERIALS

Supplementary material associated with this article can be found in the online version at doi:10.1016/j.psj.2022.101775.

REFERENCES

Abasht, B., M. B. Papah, and J. Qiu. 2021. Evidence of vascular endothelial dysfunction in Wooden Breast disorder in chickens: Insights through gene expression analysis, ultra-structural evaluation and supervised machine learning methods. PloS One 16: e0243983.

Ahmad-Nejad, P., H. Häcker, M. Rutz, S. Bauer, R. M. Vabulas, and H. Wagner. 2002. Bacterial CpG-DNA and lipopolysaccharides activate Toll-like receptors at distinct cellular compartments. Eur. J. Immunol. 32:1958–1968.

Arsenault, R. J., J. T. Lee, R. Latham, B. Carter, and M. H. Kogut. 2017. Changes in immune and metabolic gut response in broilers fed β-mannanase in β-mannan-containing diets. Poult. Sci. 96:4307–4316.

Berrong, S. L., and K. W. Washburn. 1998. Effects of genetic variation on total plasma protein, body weight gains, and body temperature responses to heat stress. Poult. Sci. 77:379–385.

Bird, A. P. 1986. CpG-rich islands and the function of DNA methylation. Nature 321:209–213.

Brownlie, R., J. Zhu, B. Allan, G. K. Mutwiri, L. A. Babiuk, A. Potter, and P. Griebel. 2009. Chicken TLR21 acts as a functional homologue to mammalian TLR9 in the recognition of CpG oligodeoxynucleotides. Mol. Immunol. 46:3163–3170.

Chang, C.-H., J. D. Curtis, L. B. Maggi, B. Faubert, A. V. Villarino, D. O'Sullivan, S. C.-C. Huang, G. J. W. van der Windt, J. Blagih, J. Qiu, J. D. Weber, E. J. Pearce, R. G. Jones, and E. L. Pearce. 2013. Posttranscriptional control of T cell effector function by aerobic glycolysis. Cell 153:1239–1251.

Cheema, M., M. Qureshi, and G. Havenstein. 2003. A comparison of the immune response of a 2001 commercial broiler with a 1957 random bred broiler strain when fed representative 1957 and 2001 broiler diets. Poult. Sci. 82:1519–1529.

Collins, K. E., H. L. Marks, S. E. Aggrey, M. P. Lacy, and J. L. Wilson. 2016. History of the Athens Canadian Random Bred and the Athens Random Bred control populations. Poult. Sci. 95:997–1004.

Cooper, K. K., J. G. Songer, and F. A. Uzal. 2013. Diagnosing clostridial enteric disease in poultry. J. Vet. Diagn. Invest. 25:314–327.

Gerriets, V. A., and J. C. Rathmell. 2012. Metabolic pathways in T cell fate and function. Trends Immunol 33:168–173.

Harrington, L. S., G. M. Findlay, and R. F. Lamb. 2005. Restraining PI3K: mTOR signalling goes back to the membrane. Trends Biochem. Sci. 30:35–42.

Havenstein, G., P. Ferket, and M. Qureshi. 2003. Carcass composition and yield of 1957 versus 2001 broilers when fed representative 1957 and 2001 broiler diets. Poult. Sci. 82:1509–1518.

He, H., T. L. Crippen, M. B. Farnell, and M. H. Kogut. 2003. Identification of CpG oligodeoxynucleotide motifs that stimulate nitric oxide and cytokine production in avian macrophage and peripheral blood mononuclear cells. Dev. Comp. Immunol. 27:621–627.

He, H., V. K. Lowry, C. L. Swaggerty, P. J. Ferro, and M. H. Kogut. 2005. In vitro activation of chicken leukocytes and in vivo protection against Salmonella enteritidis organ invasion and peritoneal S. enteritidis infection-induced mortality in neonatal chickens by immunostimulatory CpG oligodeoxynucleotide. FEMS Immunol. Med. Microbiol. 43:81–89.

Helmboldt, C. F., and E. S. Bryant. 1971. The pathology of necrotic enteritis in domestic fowl. Avian Dis 15:775–780.

Hemmi, H., O. Takeuchi, T. Kawai, T. Kaisho, S. Sato, H. Sanjo, M. Matsumoto, K. Hoshino, H. Wagner, K. Takeda, and S. Akira. 2000. A toll-like receptor recognizes bacterial DNA. Nature 408:740–745.

Henchion, M., M. Hayes, A. M. Mullen, M. Fenelon, and B. Tiwari. 2017. Future protein supply and demand: strategies and factors influencing a sustainable equilibrium. Foods 6:53.

Hogan, P. G., L. Chen, J. Nardone, and A. Rao. 2003. Transcriptional regulation by calcium, calcineurin, and NFAT. Genes Dev 17:2205–2232.

Hornbeck, P. V., B. Zhang, B. Murray, J. M. Kornhauser, V. Latham, and E. Skrzypek. 2015. PhosphoSitePlus, 2014: mutations, PTMs and recalibrations. Nucleic Acids Res 43:D512–D520.

Inoki, K., Y. Li, T. Zhu, J. Wu, and K.-L. Guan. 2002. TSC2 is phosphorylated and inhibited by Akt and suppresses mTOR signalling. Nat. Cell Biol. 4:648–657.

Jackson, S., and J. Diamond. 1996. Metabolic and digestive responses to artificial selection in chickens. Evolution 50:1638–1650.

Julian, R. J. 1998. Rapid growth problems: ascites and skeletal deformities in broilers. Poult. Sci. 77:1773–1780.

Kanehisa, M., M. Furumichi, M. Tanabe, Y. Sato, and K. Morishima. 2017. KEGG: new perspectives on genomes, pathways, diseases and drugs. Nucleic Acids Res 45:D353–D361.

Kawai, T., and S. Akira. 2006. TLR signaling. Cell Death Differ 13:816–825.

Klasing, K. C. 2007. Nutrition and the immune system. Br. Poult. Sci. 48:525–537.

Klasing, K. C., D. E. Laurin, R. K. Peng, and D. M. Fry. 1987. Immunologically mediated growth depression in chicks: Influence of feed intake, corticosterone and interleukin-1. J. Nutr. 117:1629–1637.

Kogut, M. H., and R. J. Arsenault. 2016. Editorial: Gut health: the new paradigm in food animal production. Front. Vet. Sci. 3:1–4.

Kogut, M. H., L. Rothwell, and P. Kaiser. 2003. Differential regulation of cytokine gene expression by avian heterophils during receptor-mediated phagocytosis of opsonized and oonopsonized Salmonella enteritidis. J. Interferon Cytokine Res. 23:319–327.

Krieg, A. M. 1996. Lymphocyte activation by CpG dinucleotide motifs in prokaryotic DNA. Trends Microbiol 4:73–77.

Kuttappan, V. A., B. M. Hargis, and C. M. Owens. 2016. White striping and woody breast myopathies in the modern poultry industry: a review. Poul. Sci. 95:2724–2733.

Li, S., A. D. Couvillon, B. B. Brasher, and R. A. Van Etten. 2001. Tyrosine phosphorylation of Grb2 by Bcr/Abl and epidermal growth factor receptor: a novel regulatory mechanism for tyrosine kinase signaling. EMBO J 20:6793–6804.

Macián, F., C. López-Rodríguez, and A. Rao. 2001. Partners in transcription: NFAT and AP-1. Oncogene 20:2476–2489.

Michalek, R. D., V. A. Gerriets, S. R. Jacobs, A. N. Macintyre, N. J. MacIver, E. F. Mason, S. A. Sullivan, A. G. Nichols, and J. C. Rathmell. 2011. Cutting edge: distinct glycolytic and lipid oxidative metabolic programs are essential for effector and regulatory CD4+ T cell subsets. J. Immunol. 186:3299–3303.

Moral, M. G. D., J. Fonfría, A. Varas, E. Jiménez, J. Moreno, and A. G. Zapata. 1998. Appearance and development of lymphoid cells in the chicken (Gallus gallus) caecal tonsil. Anat. Rec. 250:182–189.

Oláh, I., N. Nagy, and L. Vervelde. 2014. Chapter 2 - Structure of the avian lymphoid system. Pages 11−44 in Avian Immunology. K. A. Schat, B. Kaspers and P. Kaiser, eds. 2nd ed. Academic Press, Boston, MA.

Olkowski, A. A. 2007. Pathophysiology of heart failure in broiler chickens: structural, biochemical, and molecular characteristics. Poult. Sci. 86:999–1005.

O'Neill, L. A. J., and D. G. Hardie. 2013. Metabolism of inflammation limited by AMPK and pseudo-starvation. Nature 493:346–355.

Qureshi, M. 2003. Avian macrophage and immune response: an overview. Poult. Sci. 82:691–698.

Rodríguez-Prados, J.-C., P. G. Través, J. Cuenca, D. Rico, J. Aragonés, P. Martín-Sanz, M. Cascante, and L. Boscá. 2010. Substrate fate in activated macrophages: a comparison between innate, classic, and alternative activation. J. Immunol. 185:605–614.

Scheele, C. W. 1997. Pathological changes in metabolism of poultry related to increasing production levels. Vet. Q. 19:127–130.

Schmidt, C. J., M. E. Persia, E. Feierstein, B. Kingham, and W. W. Saylor. 2009. Comparison of a modern broiler line and a heritage line unselected since the 1950s. Poult. Sci. 88:2610–2619.

Suzuki, T., N. Yoshinaga, and S. Tanabe. 2011. Interleukin-6 (IL-6) regulates claudin-2 expression and tight junction permeability in intestinal epithelium. J. Biol. Chem. 286:31263–31271.

Szklarczyk, D., A. Franceschini, S. Wyder, K. Forslund, D. Heller, J. Huerta-Cepas, M. Simonovic, A. Roth, A. Santos, K. P. Tsafou, M. Kuhn, P. Bork, L. J. Jensen, and C. von Mering. 2015. STRING v10: protein−protein interaction networks, integrated over the tree of life. Nucleic Acids Res 43:D447–D452.

Tremblay, F., and A. Marette. 2001. Amino acid and insulin signaling via the mTOR/p70S6 kinase pathway: a negative feedback mechanism leading to insulin resistance in skeletal muscle cells. J. Biol. Chem. 276:38052–38060.

Trost, B., J. Kindrachuk, P. Määttänen, S. Napper, and A. Kusalik. 2013. PIIKA 2: an expanded, web-based platform for analysis of kinome microarray data. PLOS One 8:e80837.

Turpaev, K. T. 2006. Role of transcription factor AP-1 in integration of cell signaling systems. Mol. Biol. 40:851–866.

Vleugels, B., C. Ververken, and B. Goddeeris. 2002. Stimulatory effect of CpG sequences on humoral response in chickens. Poult. Sci. 81:1317–1321.

Wershil, B. K., and G. T. Furuta. 2008. 4. Gastrointestinal mucosal immunity. J. Allergy Clin. Immunol. 121:S380–S383.

Zhang, H. H., A. I. Lipovsky, C. C. Dibble, M. Sahin, and B. D. Manning. 2006. S6K1 regulates GSK3 under conditions of mTOR-dependent feedback inhibition of Akt. Mol. Cell 24:185–197.

Zhang, X., K. V. To, T. R. Jarvis, Y. L. Campbell, J. D. Hendrix, S. P. Suman, S. Li, D. S. Antonelo, W. Zhai, J. Chen, and H. Zhu. 2021. Broiler genetics influences proteome profiles of normal and woody breast muscle. Poult. Sci. 100:100994.

Zimmermann, S., O. Egeter, S. Hausmann, G. B. Lipford, M. Röcken, H. Wagner, and K. Heeg. 1998. Cutting edge: CpG oligodeoxynucleotides trigger protective and curative Th1 responses in lethal murine Leishmaniasis. J. Immunol. 160:3627–3630.